Separation Science and Technology
Publication details, including instructions for authors and subscription information:
http://www.informaworld.com/smpp/title~content=t713708471

Stagewise Liquid-Liquid Extraction Parametric Pumping. Equilibrium Analysis and Experiments

Denis Rachez[ab]; Gerard Delaveau[a]; Georges Grevillot[a]; Daniel Tondeur[a]
[a] LABORATOIRE DES SCIENCES DU GENIE CHIMIQUE CNRS ENSIC, NANCY, FRANCE [b] Centre de Recherches Rhone-Poulenc, Decines, France

To cite this Article Rachez, Denis , Delaveau, Gerard , Grevillot, Georges and Tondeur, Daniel(1982) 'Stagewise Liquid-Liquid Extraction Parametric Pumping. Equilibrium Analysis and Experiments', Separation Science and Technology, 17: 4, 589 — 619
To link to this Article: DOI: 10.1080/01496398208060260
URL: http://dx.doi.org/10.1080/01496398208060260

SEPARATION SCIENCE AND TECHNOLOGY, 17(4), pp. 589–619, 1982

Stagewise Liquid–Liquid Extraction Parametric Pumping. Equilibrium Analysis and Experiments

DENIS RACHEZ,* GERARD DELAVEAU, GEORGES GREVILLOT, and DANIEL TONDEUR†

LABORATOIRE DES SCIENCES DU GENIE CHIMIQUE
CNRS ENSIC
54042 NANCY, FRANCE

Abstract

A staged contacting device adapted from Craig's countercurrent extractor has been designed to allow back and forth stepwise displacement of the light liquid phase while the heavy liquid phase remains stationary. Thermal parametric pumping experiments were run in this staged apparatus, at total reflux, with water as the heavy, stationary phase, toluene as the light moving phase, and phenol as the solute distributed linearly between the two phases. The transient and steady regimes of this operation are investigated by introducing a matrix formalism and studying the properties of eigenvalues and eigenvectors. It is shown how this formalism can be extended to more complex situations involving nonideal separations and transfer of phases, several transfers per half-cycle, and partial reflux.

1. INTRODUCTION

Parametric pumping is a separation technique based on the shift of the equilibrium distribution of solutes between two phases with a thermodynamic parameter, such as pressure, pH, and most often temperature. Figure 1 illustrates schematically, for the system "water–toluene–phenol" investigated here, that by heating the mixture from 20 to 60°C, phenol is transferred from the water to the toluene phase. When a relative movement of the two phases is synchronized with the periodic temperature change, effluents of different compositions are observed at the extremities of the contacting apparatus.

This technique has been widely investigated with a fixed packed bed of adsorbent or ion exchanger being one of the phases (Refs. *1–4*, for example).

*Present address: Centre de Recherches Rhone-Poulenc, 69150 Decines, France.

†To whom correspondence should be addressed.

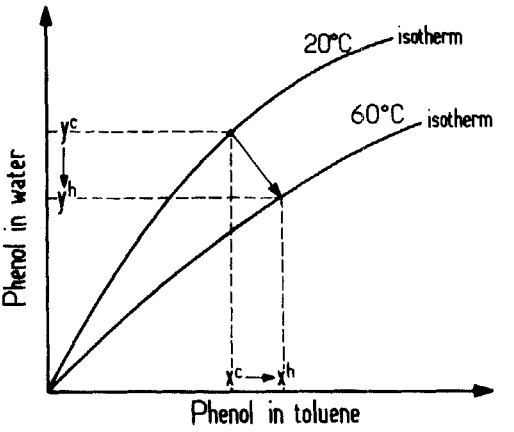

FIG. 1. Phenol distribution between water and toluene (schematic). Heating the mixtures causes transfer of phenol from water to toluene.

The principle may be extended from solid–liquid to liquid–liquid equilibria, from continuous packed beds to staged arrangements, and from continuous flow to discrete transfer to discrete fractions of the phases, and it is the purpose of the present paper to illustrate, experimentally and theoretically, this triple transposition. The only previous experiments along these lines have been presented by Wankat (5), together with an extensive numerical investigation. The first stage model of parametric pumping was presented by Wakao (*6*), and later extensively studied by Grevillot and Tondeur (*7–9*), emphasizing the analogy with distillation at steady state.

Here, we propose a contribution comprising what we believe are three original elements:

(a) A contacting device adapted from Craig's extractor (*10–19*) which makes the discrete and stagewise liquid-liquid operation convenient.

(b) Experiments with the above apparatus on the system water–toluene–phenol, so far not investigated with respect to parametric pumping.

(c) A mathematical formalism based on elementary matrix algebra, which is well adapted to such stagewise transient operations.

2. THE DISCRETE TRANSFER STAGED PARAMETRIC PUMP

Figure 2 shows the principle of the discrete transfers and equilibrations in a three-stage, total reflux parapump, with a single transfer per half-cycle. Figure 3 shows a perspective view of the device used for the experiments (which has in reality five stages). It consists of a cascade of Craig tubes, but each equipped symmetrically with two transfer reservoirs [classical Craig tubes involve only one such reservoir, and allow transfer in one direction only

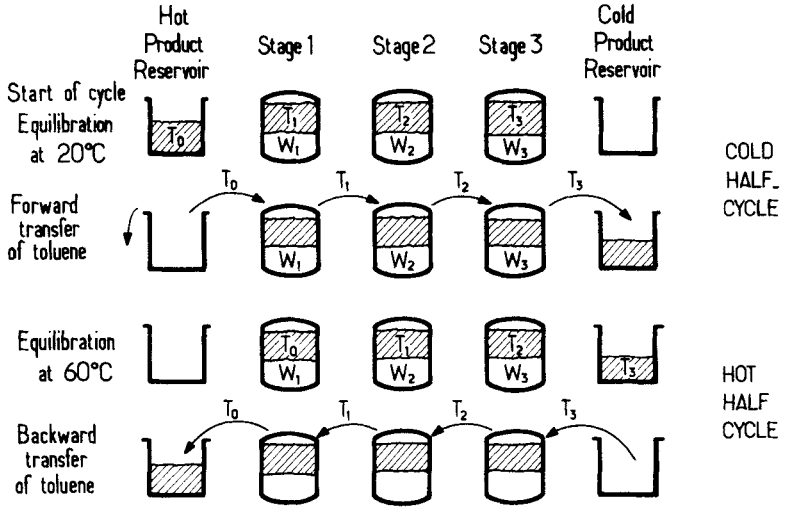

FIG. 2. Flowsheet of a 3-staged total reflux parametric pump: Hatched area, toluene; open area, water. T_0, T_1, T_2, T_3: fractions of toluene, moving phase. W_1, W_2, W_3: fractions of water, stationnary phase.

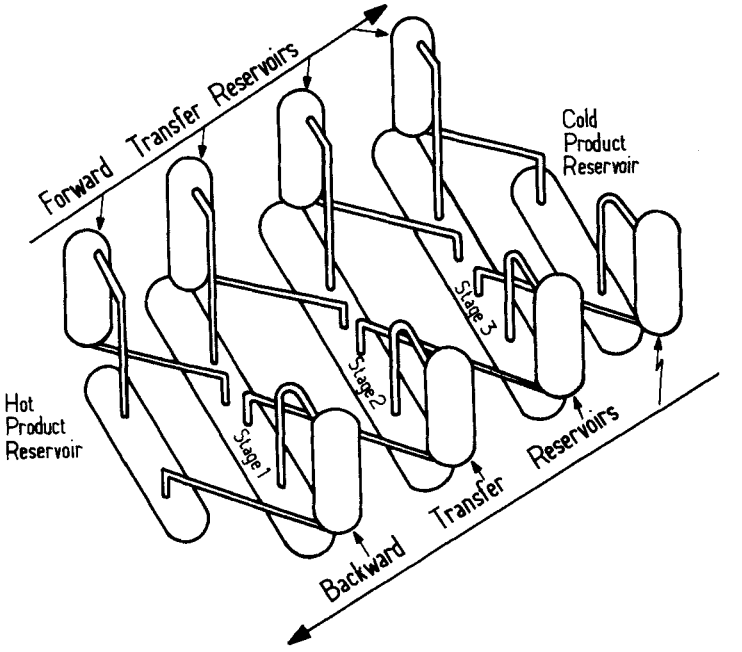

FIG. 3. Perspective view of experimental contactor (the contactor used for the experiments has five stages).

(10–19)]. The cascade comprises a product reservoir at each end, also equipped with a transfer reservoir, Stage number k is connected to the forward transfer reservoir (FTR) of stage $k - 1$ and to the backward transfer reservoir (BTR) of stage $k + 1$ through transfer tubes. When the apparatus is horizontal (stages in a horizontal plane), the transfer reservoirs are empty, and the two phases are in contact in the stages.

Figure 4 shows the principle of the transfer. When the system is tilted 90° so that the stages are vertical and the FTR's are at the bottom, the toluene phase (fraction T_k, for example) flows into the FTR. Since the latter is connected by the transfer tube to stage $k + 1$, when the system is tilted back horizontal, the toluene fraction T_k flows to stage $k + 1$ (while stage k receives fraction T_{k-1} from FTR number $k - 1$). Toluene transfer in the opposite direction (from stage k to stage $k - 1$) is obtained symmetrically by tilting the System 90° in the opposite direction so that the BTR's are at the bottom, and then back horizontal.

The tubes are made of glass and held by a metallic frame (not shown on figures) mounted on an axis to allow easy rotation for the transfers, but also to cause some agitation for better equilibration in the stages. The whole system is immerged in a tank with a thermostated water circulation. The transfer operations were done manually, and it was found simpler to carry the system from a hot tank to a cold tank rather than change the water in the same tank. Automated operation is easily conceivable. Each stage is equipped with a tapped opening (not shown on figures) which allows introduction of material and syringe withdrawals in either phase for analysis.

3. THE WATER/PHENOL/TOLUENE SYSTEM

The choice of this system was made for convenience on the basis of a rough screening of possible extractants of phenol from water likely to be sensitive to a temperature change in the range 10 to 60°C, and presenting suitable properties of low mutual solubility, low vapor pressure, density, toxicity, and cost. It is not assumed that this system is of economical interest.

The distribution isotherms of phenol between water and toluene, shown in Fig. 5, were determined at 20 and 60°C by batch equilibrations in agitated thermostated vessels. The analyses were done by gas chromatography (FID detector) on a Porapak column around 230°C with 1 μL injections. The isotherms may reasonably be assumed linear in the range 0–2 g/L in toluene, but the curvature becomes noticeable above 3 g/L. Equilibrium determinations were also made during the experiments, when the cold temperature was below 20°C.

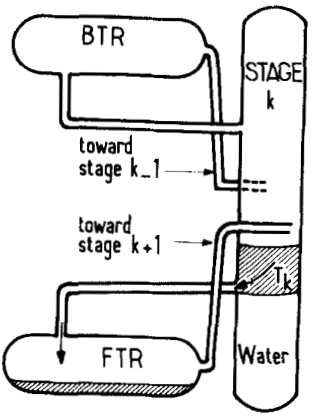

FIG. 4. Illustration of toluene transfer mechanism in contacting apparatus.

4. FORMAL MATHEMATICAL SOLUTION

Let $x_j^c(n)$ designate the phenol concentration, in grams per liter, in toluene fraction number j ($j = 0, 1, \ldots, N$) at the cold temperature during cycle n. Similarly, $y_k^h(n)$ designates the phenol concentration in the water phase at the hot temperature in stage k ($k = 1, 2, \ldots, N$) during cycle n. N designates the total number of stages; the number of toluene fractions is thus $N + 1$. With these notations, at the start of cycle n (as represented on Fig. 2), $x_0^c(n)$ is the

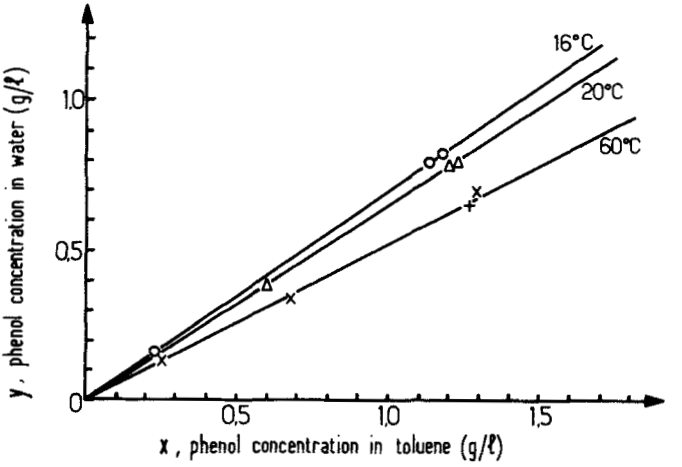

FIG. 5. Distribution equilibria of phenol between water and toluene at 16, 20, and 60°C.

concentration in the hot product reservoir. In stage k, $x_k^c(n)$ is in equilibrium at 20°C with $y_k^c(n)$. Let T be the volume of the toluene fractions assumed equal and constant, and W be the volume of the water fractions, also assumed equal and constant.

We shall establish a relation between the concentrations in cycle n and cycle $n+1$. To do this, we first write material balances and equilibrium relations within cycle n (Eqs. 1 to 7), the index (n) of the cycle being omitted for simplicity. After a forward transfer, and before any equilibration, stage k contains T toluene of concentration x_{k-1}^c and W water of concentration y_k^c. After reequilibration at 60°, these concentrations become respectively x_{k-1}^h and y_k^h. Conservation of phenol implies

$$y_k^h + \rho x_{k-1}^h = y_k^c + \rho x_{k-1}^c \qquad (k = 1, \ldots, N) \tag{1}$$

where ρ is the ratio of light to heavy phase volumes:

$$\rho = T/W \tag{2}$$

Equilibrium at 20°C at the start of the cycle, and at 60°C after forward transfer, is expressed by

$$y_k^c = \alpha^c x_k^c \qquad (k = 1, \ldots, N) \tag{3}$$

$$y_k^h = \alpha^h x_{k-1}^h \qquad (k = 1, \ldots, N) \tag{4}$$

where α^c and α^h are the slopes of the equilibrium isotherms (Fig. 5) assumed linear. When Eqs. (3) and (4) are substituted into Eq. (1), one obtains, after rearrangement,

$$x_{k-1}^h = \frac{\rho}{\rho + \alpha^h} x_{k-1}^c + \frac{\alpha^c}{\rho + \alpha^h} x_k^c \qquad (k = 1, \ldots, N) \tag{5}$$

since the last toluene fraction is in the cold product reservoir during the hot equilibration, it undergoes no exchange, thus no concentration change. Thus

$$x_N^h = x_N^c \tag{6}$$

Equations (5) and (6) form a system of $N+1$ linear difference equations relating the x^h's to the x^c's. In matrix form, this is expressed by

$$\mathbf{X}^h(n) = [\theta_h]\mathbf{X}^c(n) \tag{7}$$

where $\mathbf{X}^h$ and $\mathbf{X}^c$ are the column vectors of the toluene fraction concentrations, and $[\theta_h]$ is the $N+1$ dimensional bidiagonal matrix:

$$[\theta_h] = \frac{1}{\rho + \alpha^h} \begin{bmatrix} \rho & \alpha^c & 0 & \cdots & 0 \\ 0 & \ddots & \ddots & & \vdots \\ \vdots & & \ddots & \ddots & \\ & & & \rho & \alpha^c \\ 0 & \cdots & \cdots & 0 & (\rho + \alpha^h) \end{bmatrix} \tag{8}$$

A similar analysis for the backward half-cycle leads to a symmetrical relation between $\mathbf{X}^h(n)$ and the concentration vector $\mathbf{X}^c(n+1)$ which represents the conditions after the cold reequilibration. Thus at the beginning of cycle, $n+1$:

$$\mathbf{X}^c(n+1) = [\theta_c]\mathbf{X}^h(n) \tag{9}$$

with

$$[\theta_c] = \frac{1}{\rho + \alpha^c} \begin{bmatrix} \rho + \alpha^c & & & 0 \\ & \ddots & & \\ \alpha^h & & \rho & \\ & \ddots & & \ddots \\ 0 & & \alpha^h & \rho \end{bmatrix} \tag{10}$$

Equations (7) and (9) may be combined to yield the sought recurrence over a complete cycle:

$$\mathbf{X}^c(n+1) = [\mathbf{M}]\mathbf{X}^c(n) \tag{11}$$

where $[\mathbf{M}]$ is the tridiagonal Jacobi matrix of dimension $N+1$:

$$[\mathbf{M}] = [\theta_c][\theta_h] = \begin{bmatrix} d & e & & & \\ a & b & c & & 0 \\ a & b & c & & \\ & \ddots & \ddots & \ddots & \\ & & & \ddots & c \\ & 0 & & a & a+b \end{bmatrix} \tag{12}$$

with

$$a = \rho\alpha^h; \qquad b = \rho^2 + \alpha^c\alpha^h; \qquad c = \rho\alpha^c; \qquad d = \rho(\rho + \alpha^c); \tag{13}$$
$$e = \alpha^c(\rho + \alpha^c); \qquad p = (\rho + \alpha^c)(\rho + \alpha^h) = a + b + c$$

Equation (11) is a linear homogeneous first-order difference equation from which we have obviously:

$$\mathbf{X}^c(n) = [\mathbf{M}]\mathbf{X}(n-1) = [\mathbf{M}]^2\mathbf{X}(n-2) = \cdots = [\mathbf{M}]^n\mathbf{X}^c(0) \quad (14)$$

Equation (14) allows the concentration vector for any cycle to be obtained from the initial concentration vector $\mathbf{X}(0)$. It may thus be called a solution of the conservation equations, and this solution is formally very simple. However, the calculation of the nth power of the matrix $[\mathbf{M}]$ is not a trivial matter if its dimension and n are large. We therefore devote some attention to this calculation, which will bring further insight into the physical problem.

5. CALCULATION OF $[\mathbf{M}]^n$

The calculation of the nth power of a matrix by successive multiplication is numerically straightforward, although it may require much time and gives little qualitative information. Alternate methods require the calculation of the eigenvalues λ of $[\mathbf{M}]$ for which standard numerical methods exist. In the case at hand, much information can be obtained on the eigenvalues by algebraic means, and a simple, rapidly converging numerical method can be used (see Appendix A and Ref. *20*) owing to the fact that the matrix is of the Jacobi type (that is, tridiagonal). Once the eigenvalues λ are known, the elements of the corresponding eigenvectors are calculated directly by

$$\begin{aligned}
x_{1k} &= -\frac{1}{e}(d - p\lambda_k)x_{0k} \\
x_{2k} &= -\frac{1}{c}[(b - p\lambda_k)x_{1k} + ax_{0k}] \\
x_{jk} &= -\frac{1}{c}[(b - p\lambda_k)x_{j-1,k} + ax_{j-2,k}] \qquad (15) \\
x_{N,k} &= -\frac{1}{c}[(b - p\lambda_k)x_{N-1,k} + ax_{N-2,k}], \qquad k = 0, 1, \ldots, N
\end{aligned}$$

where a, b, c, d, e, and p are given by Eqs. (13). As usual, the elements of the eigenvectors are defined up to a multiplicative factor, here considered to be x_{0k}. Designating by $[\mathbf{P}]$ the matrix of column eigenvectors, of elements x_{jk}, the matrix $[\mathbf{M}]$ may now be written in diagonalized form:

$$[\mathbf{M}] = [\mathbf{P}][\Lambda][\mathbf{P}^{-1}] \quad (16)$$

where $[\Lambda]$ is the diagonal matrix of eigenvalues. We then have directly

$$[\mathbf{M}]^n = [\mathbf{P}][\Lambda]^n[\mathbf{P}^{-1}] \quad (17)$$

and

$$[\Lambda]^n = \begin{bmatrix} \lambda_0^n & & & 0 \\ & \lambda_1^n & & \\ & & \ddots & \\ 0 & & & \lambda_N^n \end{bmatrix} \tag{18}$$

An equivalent approach is to use Sylvester's theorem (20) which gives

$$[\mathbf{M}]^n = \sum_{j=0}^{N} \lambda_j^n [\mathbf{A}_j] \tag{19}$$

where

$$[\mathbf{A}_j] = \frac{\text{adj } (\lambda_j \mathbf{I} - \mathbf{M})}{\prod_{i \neq j} (\lambda_j - \lambda_i)} \tag{20}$$

and adj $(\lambda_j \mathbf{I} - \mathbf{M})$ is the transpose matrix of cofactors of $[\lambda_j \mathbf{I} - \mathbf{M}]$, independent of n. It is seen that the number of cycles n appears only as the powers of the eigenvalues, and this allows a quick qualitative look on how the system converges toward its steady state. Here, we shall first try to characterize this steady state.

6. THE CYCLIC STEADY STATE

The behavior of the system when the number of cycles n becomes large can be deduced from a close examination of Eqs. (16) to (20) and of the eigenvalues, but also induced from physical reasoning. In Appendix A we demonstrate that all eigenvalues of $[\mathbf{M}]$ are real, positive, and smaller than or equal to 1. We thus have

$$0 < \lambda_0 < \lambda_1 < \cdots < \lambda_N = 1 \tag{21}$$

These conclusions are consistent with the following intuitive considerations:

Any negative eigenvalue would bring a contribution to $[\mathbf{M}]^n$ that changes sign every cycle, leading to an oscillatory behavior of certain concentrations. Such a behavior is incompatible with the properties of linear systems.

Any eigenvalue larger than 1 would lead to an ever-increasing contribution to $[\mathbf{M}]^n$, and to infinite concentrations.

Any eigenvalue positive but smaller than 1 has an ever-decreasing contribution as n becomes large. If there were no eigenvalue equal to 1, $[\mathbf{M}]^n$ would tend toward the zero matrix, and all final concentrations would be zero.

Note that this reasoning in no way constitutes a mathematical proof, and should rather be taken as an indication that the mathematical problem is well posed.

From Eqs. (14), (19), and (20), when n becomes large, the contribution of all eigenvalues different from one disappear and the cyclic steady state is given by

$$\mathbf{X}^c(\infty) = [\mathbf{M}]^\infty \mathbf{X}^c(0) = \frac{[\text{adj}\,(\mathbf{I} - \mathbf{M})]}{\prod_{i \neq N} (1 - \lambda_i)} \mathbf{X}^c(0) \tag{22}$$

More explicit information is obtained by noting that, in the steady state, we must have

$$\mathbf{X}^c(n + 1) = \mathbf{X}^c(n) = \mathbf{X}^c(\infty) \tag{23}$$

and that this equality is compatible with Eq. (11) only if $\mathbf{X}^c(\infty)$ is an eigenvector of matrix $[\mathbf{M}]$. From the discussion above, it must be the eigenvector corresponding to $\lambda_N = 1$. Thus the components x_i^* of $\mathbf{X}^c(\infty)$ are calculated by letting $\lambda_k = \lambda_N = 1$ in the set of Eqs. (15). It may easily be verified that the following relations hold between the concentrations x^* thus calculated:

$$\frac{x_0^*}{x_1^*} = \frac{x_1^*}{x_2^*} = \cdots \frac{x_j^*}{x_{j+1}^*} = \cdots \frac{x_{N-1}^*}{x_N^*} = \frac{\alpha^c}{\alpha^h} = \beta \tag{24}$$

which implies

$$x_0^*/x_N^* = \beta^N \tag{25}$$

This is the equivalent of Fenske's equation, already established in Ref. 9. The steady-state composition vector may then be written, in terms of x_0^*, for example:

$$\mathbf{X}^c(\infty) = \begin{vmatrix} x_0^* \\ x_1^* \\ \cdot \\ \cdot \\ \cdot \\ x_N^* \end{vmatrix} = x_0^* \begin{bmatrix} 1 \\ \beta^{-1} \\ \beta^{-2} \\ \cdot \\ \cdot \\ \cdot \\ \beta^{-N} \end{bmatrix} \tag{26}$$

An interesting property of this vector is that it is invariant upon multiplication on the left by $[\theta_h]$ which, from Eq. (7), entails that

$$\mathbf{X}^h(\infty) = \mathbf{X}^c(\infty) \tag{27}$$

This means that the compositions of the toluene fractions are the same after an equilibration at 60 and at 20°C. In other words, in the cyclic steady state, all compositions are constant, and no phenol transfer occurs between phases.

The geometric interpretation of Relations (24) to (27) in a McCabe-Thiele-like diagram is a staircase construction between two straight lines, as shown in Figs. 6a and 6b, and is consistent with previous studies (*6–9*). The steady-state composition vector in Eq. (26) is defined up to the value of x_0^*. This parameter (the phenol concentration in toluene fraction T_0, in the hot product Resevoir) is calculated from an overall material balance over the system to give (see Appendix B)

$$x_0^* = \frac{Q/W}{\rho + (\rho + \alpha^c)\sum_{i=1}^{N} \beta^{-i}} \tag{28}$$

This result is seen to be independent of the initial distribution but to depend only on Q, the total mass of phenol present in the system.

The knowledge of this steady state allows determination of the structure of $[\mathbf{M}]^n$ when n becomes large, as illustrated in Appendix B.

7. EXAMPLE OF ANALYSIS OF TRANSIENT REGIME

The equilibrium isotherms (Fig. 5) are characterized by the following values of the slopes

At 16°C: $\alpha^c = 0.70$,

$$\beta = \frac{\alpha^c}{\alpha^h} = 1.346$$

At 60°C: $\alpha^h = 0.52$,

This corresponds to the experimental conditions of Run 1. We have also

$$\rho = \frac{T}{W} = \frac{26 \text{ mL toluene}}{26 \text{ mL water}} = 1$$

and $N = 5$ since there are five stages. With these values, the matrix $[\mathbf{M}]$ is written (Eqs. 12 and 13)

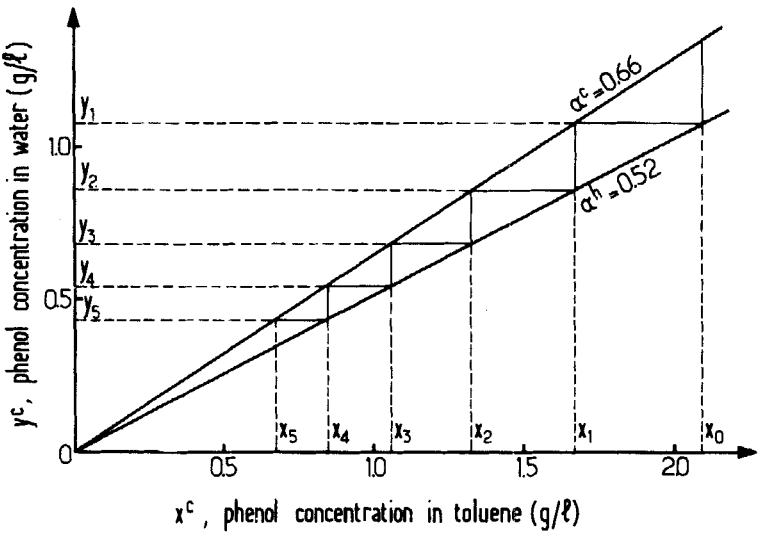

FIG. 6a. Relation between mobile phase and stationary phase compositions at the low temperature in cyclic steady state (conditions of Run 2).

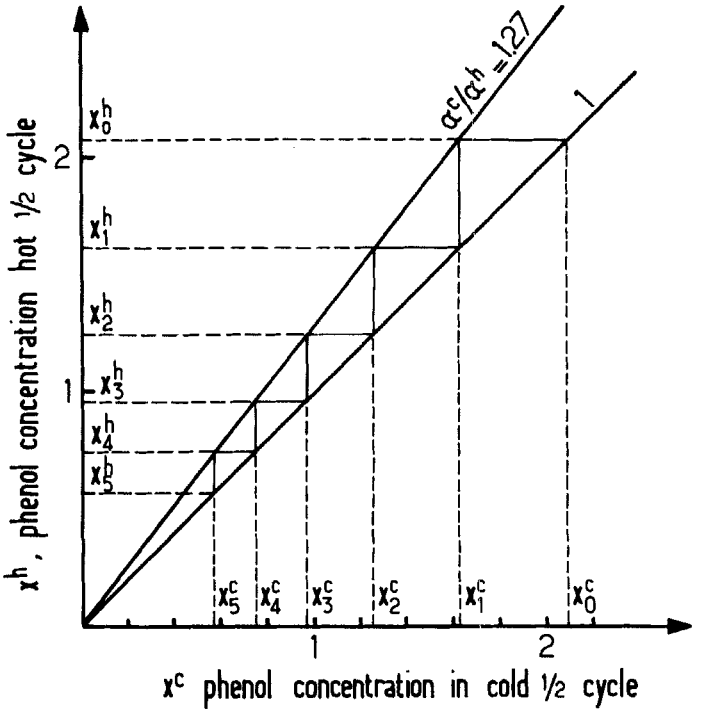

FIG. 6b. Relation between compositions in mobile phase in the hot and cold half-cycle in cyclic steady state (conditions of Run 2).

$$[\mathbf{M}] = \frac{1}{2.584}\begin{bmatrix} 1.70 & 1.19 & 0 & 0 & 0 & 0 \\ 0.52 & 1.364 & 0.70 & 0 & 0 & 0 \\ 0 & 0.52 & 1.364 & 0.70 & 0 & 0 \\ 0 & 0 & 0.52 & 1.364 & 0.70 & 0 \\ 0 & 0 & 0 & 0.52 & 1.364 & 0.70 \\ 0 & 0 & 0 & 0 & 0.52 & 1.884 \end{bmatrix}$$

The eigenvalues, calculated as outlined in Section 5, are

$$\begin{aligned} \lambda_0 &= 0.1050 \\ \lambda_1 &= 0.2522 \\ \lambda_2 &= 0.4838 \\ \lambda_3 &= 0.7336 \\ \lambda_4 &= 0.9239 \\ \lambda_5 &= 1.0000 \end{aligned}$$

These calculations were performed with eight significant figures.

In Run 1, the initial condition is that all toluene fractions are identical and in equilibrium with the water fractions with the following phenol concentrations ($i = 0, 1, \ldots, N$):

$$\left.\begin{aligned} q = x_i(0) &= 1.18 \text{ g phenol/L toluene} \\ y_i(0) &= 0.826 \text{ g phenol/L water} \end{aligned}\right\} \quad \text{at equilibrium at } 16^\circ\text{C}$$

so that the total amount of phenol is

$$Q = 0.290 \text{ g phenol}$$

Then from Eq. (28) we calculate

$$x_0^* = 2.324 \text{ g phenol/L toluene}$$

The final steady state is then given by Eq. (26):

$$\mathbf{X}^c(\infty) = \begin{bmatrix} x_0^* = 2.324 \\ x_1^* = 1.726 \\ x_2^* = 1.282 \\ x_3^* = 0.953 \\ x_4^* = 0.708 \\ x_5^* = 0.526 \end{bmatrix}$$

Now, we should like to know the composition at an arbitrary cycle n. In principle, we would have to calculate $[\mathbf{P}^{-1}]$ in order to use Eqs. (17) and (18) or calculate the $[\mathbf{A}_j]$ in order to use Eqs. (19) and (20). We shall see that these tedious calculations may be partly avoided if only estimations are

sought and for n sufficiently large. Equation (17) or (19), when developed, leads to expressions of the form

$$\mathbf{X}^c(n) = \begin{vmatrix} a_{00}\lambda_0^n + a_{01}\lambda_1^n + a_{02}\lambda_2^n + a_{03}\lambda_3^n + a_{04}\lambda_4^n + x_0^* \\ a_{10}\lambda_0^n + a_{11}\lambda_1^n + \cdots\cdots\cdots\cdots + x_1^* \\ a_{20}\lambda_0^n + \cdots\cdots\cdots\cdots\cdots\cdots + x_2^* \\ a_{30}\lambda_0^n \\ a_{40}\lambda_0^n \\ a_{50}\lambda_0^n \cdots\cdots\cdots\cdots\cdots\cdots + x_N^* \end{vmatrix}$$

the last column corresponds to $\mathbf{X}^c(\infty)$. Examination of the successive powers of the λ's shows that the contribution of the smallest eigenvalues rapidly becomes negligible. This is illustrated on Fig. 7 where $\ln \lambda_i^n$ is plotted against n. We observe that λ_0^n becomes negligible with respect to 1 ($\lambda_0^n < 10^{-3}$) as early as the third cycle, λ_1^n around the fifth cycle, and λ_2^n around the tenth cycle. The contribution of λ_3 persists until the 20th cycle, and that of λ_4 until the 90th cycle. These contributions are somewhat modified by the factors a_{ij}, but these actually reinforce the importance of the largest eigenvalues. Figure 8a shows a comparison between the rigorous curve (full line) and the approximation obtained by neglecting the contributions of λ_1, λ_2, λ_3. This relation is expressed by

$$\mathbf{X}(n) - \mathbf{X}(\infty) = q\mathbf{C}\lambda_4^n \tag{29}$$

with

$$\mathbf{C} = \begin{vmatrix} -1.024 \\ -0.563 \\ -0.090 \\ +0.339 \\ +0.540 \\ +0.615 \end{vmatrix} \qquad \text{and } q = 1.18 \text{ g/L}$$

It is seen that this approximation, besides showing the correct trend, gives an estimate better than 10% for $n \geq 3$, better than 5% for $n \geq 10$, and better than 1% for $n \geq 20$. For all practical purposes, it thus seems sufficient to calculate the matrix $[\mathbf{A}_j]$ corresponding to $\lambda_j = \lambda_4$ in Eq. (19) or, in other terms, to calculate the two lines in $[\mathbf{P}^{-1}]$ that correspond to the two largest eigenvalues.

Note that Eq. (29) is comparable to a result established by Pigford et al.

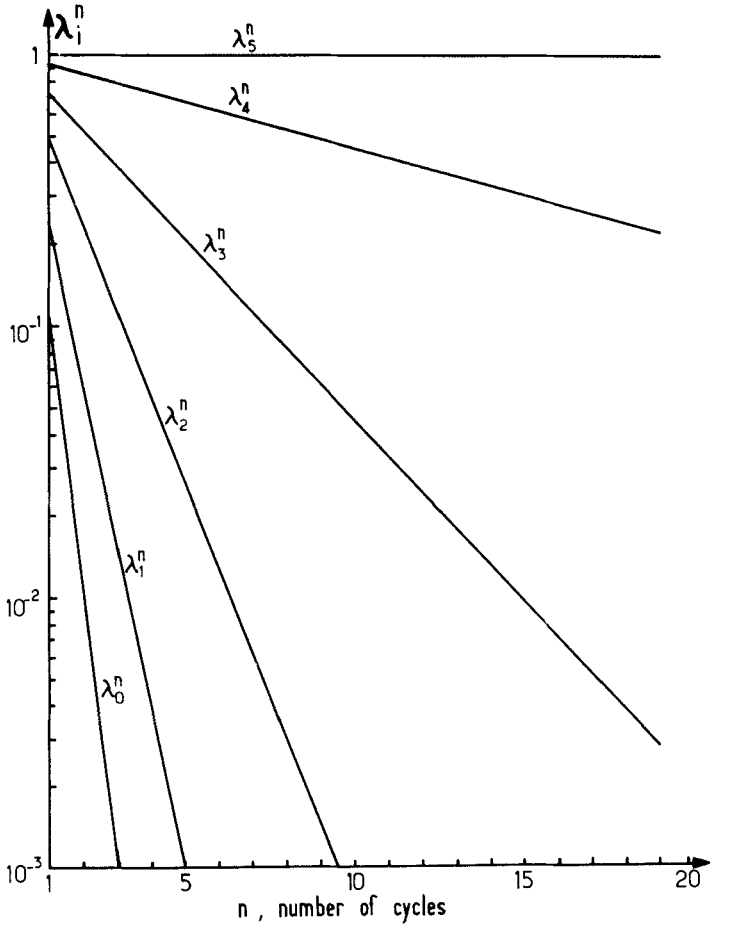

FIG. 7. Plot of λ_i^n as a function of the number of cycles n (logarithmic ordinate).

(26) for linear packed bed parapumps after a certain start-up period. Using their notation, their Eqs. (16) and (17) may be put in the form

$$(y_T)_n - (y_T)_\infty = (y_B)_n - (y_B)_\infty = \left(\frac{1-b}{1+b}\right)^n y_0$$

which expresses that the "distance" from the steady state for top and bottom reservoir concentrations is a power function of the number of cycles.

8. DISCUSSION OF EXPERIMENTAL RESULTS

Experimental Runs

The experimental procedure is that described in Sections 2 and 3.

Figures 8a and 8b show calculated curves and experimental points for the phenol concentration in the six toluene fractions, and in the five water fractions respectively, in Run 1. The measurements were made at the beginning of the cycles, after equilibration at the cold temperature, by syringe withdrawals in each phase. The conditions for Run 1 were given in the previous section. Similarly, Figs. 9a and 9b show the results of Run 2 for which the parameters are

$$\alpha^c(20°C) = 0.66 \qquad \beta = 1.27$$

$$\alpha^h(60°C) = 0.52$$

$$T = 35 \text{ mL of toluene} \qquad \rho = 1.35$$

$$W = 26 \text{ mL of water}$$

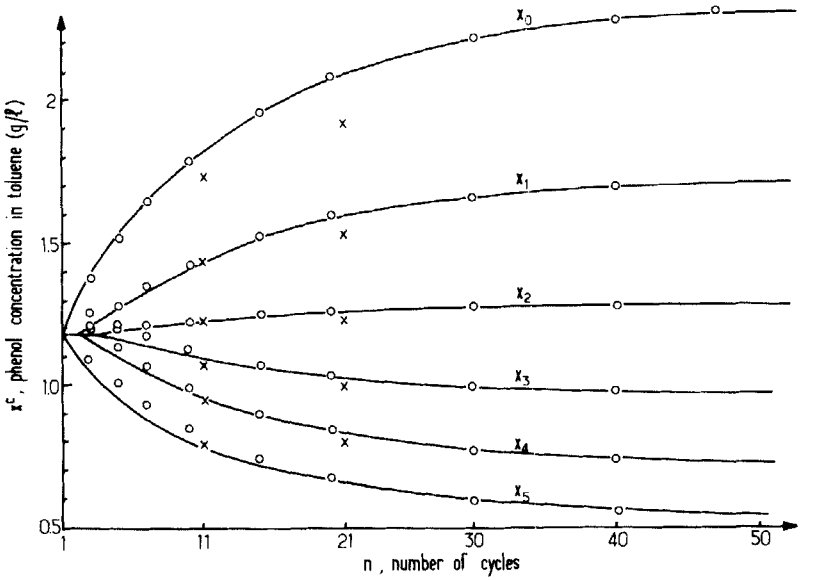

FIG. 8a. Transient regime of Run 1: Toluene phase. Rigorous solution: Full line. Highest eigenvalue approximation: (○). Experimental measurements: (×). (Concentrations are measured in the cold half-cycle.)

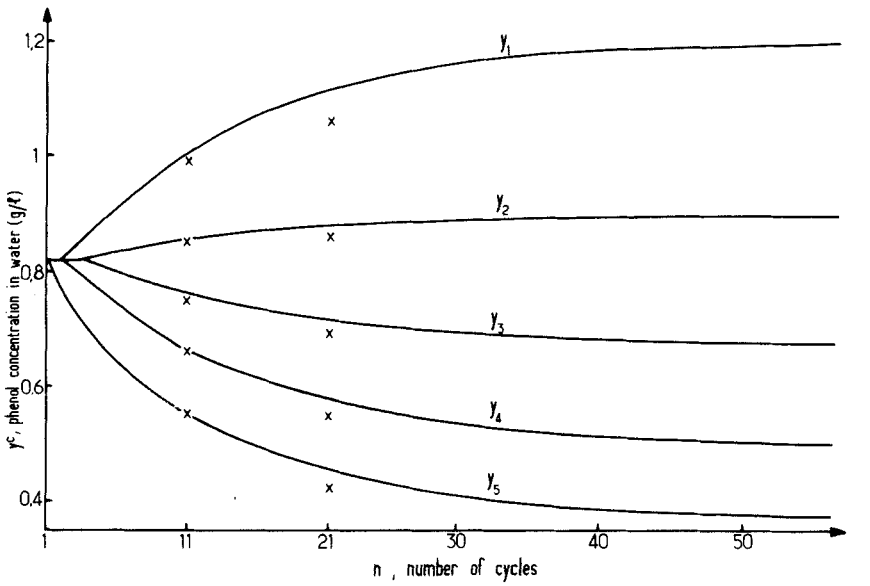

FIG. 8b. Transient regime of Run 1: Water phase. Symbols: See Fig. 8a.

As expected from the smaller value of β, the maximal separation in Run 2 is smaller than in Run 1.

Dissymetry of Light Phase Transfers

After about 10 cycles we observed that fraction T_5 of toluene had become much smaller than the others, and that fractions T_0 and T_1 had become larger. This phenomenon amplified to the point that around the 20th cycle practically no toluene was left in fraction T_5 and the experiment had to be interrupted. On the other hand, the volumes of water remained practically constant, with a slight excess in the first stages (5% difference between first and fifth stage).

A detailed analysis of the phenomena involved in the light phase transfer leads to the following:

The water level, in vertical position during transfer, is slightly below the overflow tube. This entails that no water is transferred, but about 1 cm^3 of toluene remains stationnary in each stage.

Evaporation was verified to be negligible, the system being hermetic.

The solubility difference of water in toluene between 20 and 60°C should entail a net transfer of water toward the first stages, of the order of 0.1% per

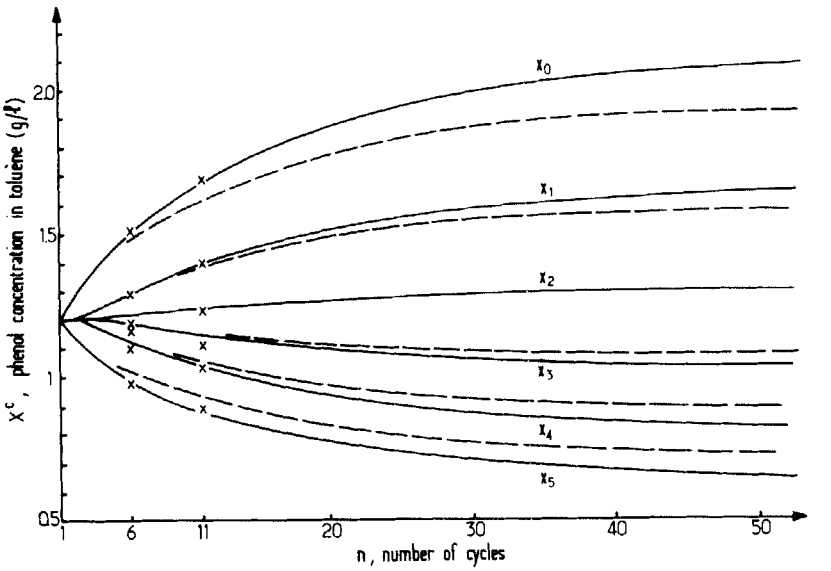

FIG. 9a. Transient regime of Run 2: Toluene phase. Calculated without dead volume: Full line. Calculated with dead fraction $\gamma = 0.1$: dashed line. Experimental Measurements: (×).

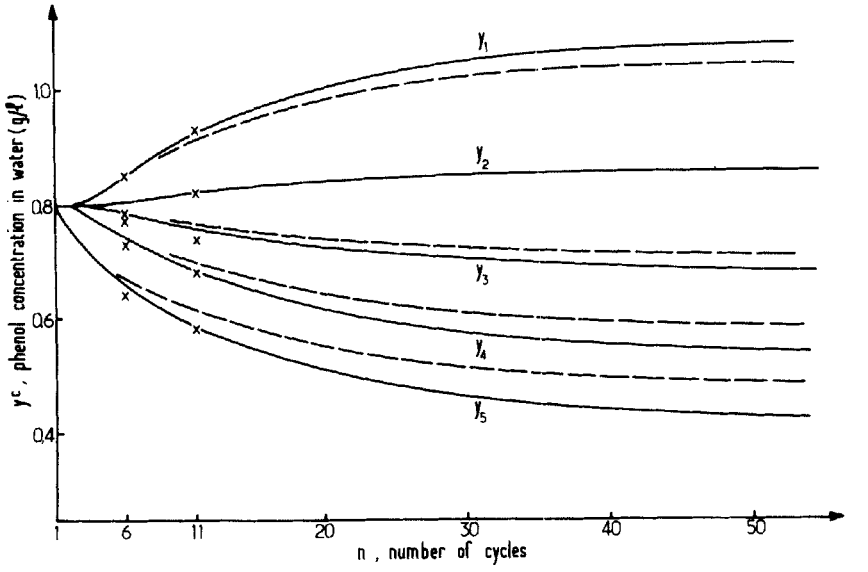

FIG. 9b. Transient regime of Run 2: Water phase. Symbols: See Fig. 9a.

cycle. This is consistent with the observation above in direction, but smaller in amplitude.

The dilatation of water from 20 and 60°C is about 1.5%, not enough to entail water transfer, but enough to entail a net transfer of toluene of the same amount at each cycle, thus 15% after 10 cycles, toward the first stages.

A slight dissymmetry of the tubes on one side can explain an important and cumulative net transfer. Suppose the volume available in the vertical position, up to the overflow tube, is smaller by 1.5% on the side of the backward transfer reservoirs. This implies an excess of toluene transfer in the backward direction, thus toward the first stages, of about 15% in 10 cycles.

The two latter effects (dilatation and dissymmetry) may explain the net transfer of toluene observed, which is in the average about 30% in 10 cycles. These effects may be in principle offset by a proper adjustment of the holdup volumes of the stages. This was tried by working the glass of the apparatus, and resulted in a net transfer of toluene in the opposite direction! It is expected that this net transfer of light phase would be a lesser problem in a partial reflux system.

Other Uncertainties

The cold source was not thermostated, and varied by 2 to 3°C during the experiments. This is expected to have a nonnegligible effect, but was not corrected for. The equilibrium determinations were delicate due to having to take samples with a syringe at two different temperatures from two different phases with different dilatation coefficients. The dilatation effects were evaluated and accounted for, but errors remain due to evaporation at 60°. The time allowed for equilibration between a temperature change and a transfer was set to 5 min after trials which indicated that no composition change was meaningfully detected after that time.

The purely analytical uncertainty (of the order of 2%) is expected to be small with respect to the uncertainty above.

Conclusion

In spite of these various uncertainties, the experimental data seem to agree reasonably with the calculations, at least for a small number of cycles (6 or 11). The more important discrepancy observed in Run 1 for 21 cycles is attributed to the volume variation of the toluene fractions (fraction T_5 had practically disappeared at Cycle 21), entailing a variation of ρ and thus of the elements of the matrix [**M**] from cycle to cycle.

9. EXTENSION OF THE THEORETICAL APPROACH

The preceding discussion illustrates that in any real experiment we would be faced with imperfect phase transfer, volume variations of the fractions, volume differences in the stages, etc. In addition, the mode of parametric pumping considered here is restrictive; it ignores partial reflux and multiple transfers per half-cycle, situations studied elsewhere (*8, 9*) from the point of view of the cyclic steady state. We should like to give a hint on how the present approach can be extended, without major difficulty, to account for some of the situations mentioned above. For this purpose we shall examine how the basic equations are altered separately by the different effects.

Existence of a Dead Volume of Light Phase

In the experiments presented, we mentioned that about 1 cm^3 of toluene was not transferred when the apparatus was tilted to the vertical position. Let us characterize this "dead volume" D by its ratio γ to the volume of the water fractions.

$$\gamma = D/W \tag{30}$$

and we suppose this ratio is constant and the same for all stages in forward and backward transfer. When the material balances (Eqs. 1) are rewritten taking this hold-up into account, one obtains the same form as Eq. (5) but with ρ replaced by $\rho - \gamma$, α^c by $\alpha^c + \gamma$ and α^h by $\alpha^h + \gamma$ (so that the denominator $\rho + \alpha^h$ in Eq. 5 is unchanged). A similar property holds for the backward half-cycle, and finally the whole approach outlined so far remains valid providing the substitutions indicated above are made in the elements of the matrix [**M**]. The discontinuous lines in Figs. 9a and 9b show the result of such a calculation, made with a 10% dead volume of solvant ($\gamma = 0.1$) which slightly overestimates reality.

Intuitively, the effect of γ can be foreseen by considering the system as having a lower ρ and higher α's but a lower effective β. The effect on the cyclic steady state is seen immediately from Fenske's equation (eq. 25), with the data of Run 2:

$$\frac{x_0^*}{x_N^*} = \beta_{\text{effective}}^5 = \left[\frac{\alpha^c + \gamma}{\alpha^h + \gamma}\right]^5 \qquad \begin{cases} = 3.29 \text{ for } \gamma = 0 \\ = 2.77 \text{ for } \gamma = 0.1 \end{cases}$$

The effect of a smaller ρ and larger α's is favorable to speed of convergence but may be offset by the decrease in β.

Unequal Volumes of Fractions

A simple modification accounts for the volume of water being different in each stage and the volumes of each toluene fraction being different, providing these volumes are constant (same volume transferred back and forth). It suffices to take a different ρ_k for each stage and for equilibrations at different temperatures. In the forward matrix $[\theta_h]$ (Eq. 8), the unique ρ will be replaced by ρ_k^h, different in each line, and similarly, in matrix $[\theta_c]$, ρ_k^c will be introduced. The product matrix $[\mathbf{M}]$ remains tridiagonal, and the methods for eigenvalues and eigenvector calculations are unchanged. All the other properties mentioned still hold.

Volume Variations of Phases

As discussed earlier, important variations of the volume of the toluene fractions may be caused by a geometric dissymmetry of the apparatus in forward versus backward transfer and by dilatation of the water phase. These effects can be quantified and accounted for in writing the material balances. Unfortunately, they will cause the value of ρ to change in each stage and *at each cycle*. There is therefore no unique matrix $[\mathbf{M}]$ and the approach presented fails to apply.

Several Transfers per Half-Cycle

Suppose the apparatus used in the present work was equipped with an additional reservoir in series at each end. Then seven toluene fractions would be used, and there would be two successive transfers in the same direction at each temperature. The cyclic steady state of such systems has been extensively studied (*8*). The matrix formalism can be used conveniently by noting that each transfer of light phase followed by an equilibration is described by a bidiagnoal matrix similar to $[\theta_c]$ or $[\theta_h]$. Let us consider for example a parapump with two stages and four light phase fractions, thus two transfers per half-cycle. By an approach similar to that leading to Eq. (11), it is shown that the matrix $[\mathbf{M}]$ describing the complete cycle is the product of the successive bidiagonal matrices describing each transfer:

$$[\mathbf{M}] = [\theta_{c2}][\theta_{c1}][\theta_{h2}][\theta_{h1}] \tag{31}$$

where

$$[\theta_{c2}] = \frac{1}{\rho + \alpha^c} \begin{bmatrix} \rho + \alpha^c & 0 & 0 & 0 \\ 0 & \rho + \alpha^c & 0 & 0 \\ 0 & \alpha^h & \rho & 0 \\ 0 & 0 & \alpha^h & \rho \end{bmatrix} \quad [\theta_{c1}] = \frac{1}{\rho + \alpha^h} \begin{bmatrix} \rho + \alpha^h & 0 & 0 & 0 \\ \alpha^h & \rho & 0 & 0 \\ 0 & \alpha^h & \rho & 0 \\ 0 & 0 & 0 & \rho + \alpha^h \end{bmatrix}$$

$$[\theta_{h2}] = \frac{1}{\rho + \alpha^h} \begin{bmatrix} \rho & \alpha^c & 0 & 0 \\ 0 & \rho & \alpha^c & 0 \\ 0 & 0 & \rho + \alpha^h & 0 \\ 0 & 0 & 0 & \rho + \alpha^h \end{bmatrix} \quad [\theta_{h1}] = \frac{1}{\rho + \alpha^c} \begin{bmatrix} \rho + \alpha^c & 0 & 0 & 0 \\ 0 & \rho & \alpha^c & 0 \\ 0 & 0 & \rho & \alpha^c \\ 0 & 0 & 0 & \rho + \alpha^c \end{bmatrix}$$

[**M**] is no longer tridiagonal but, in the present case, comprises five diagonals. The simple numerical methods for calculating eigenvalues and eigenvectors of tridiagonal matrices no longer apply, but otherwise the general method is unchanged. Notice also that different definitions of [**M**] may be introduced, depending on how the beginning of the cycle is defined. These various forms differ from each other by a circular permutation on the bidiagonal matrices $[\theta]$.

Partial Reflux Parapump

We adopt the description given by Grevillot (*9*) for one transfer per half-cycle in a pump where fresh feed is added at each half-cycle in an intermediate stage and with a different reflux ratio at each end. The operating scheme of such a pump is summarized on Fig. 10. The equations describing the operation of the lower section during the cold half-cycle and the upper section during the hot half-cycle are that of the simplest case; that is, Eqs. (1) to (10). The other equations are those for a hold-up γ in each stage, as explained in a previous paragraph (ρ replaced by $\rho - \gamma$, α by $\alpha + \gamma$). Special material balances must be written for the feed stage. The result may be written in the following form:

$$\mathbf{X}^h(n) = [\theta_h]\mathbf{X}^c(n) + \mathbf{F}_h \tag{32}$$

$$\mathbf{X}^c(n+1) = [\theta_c]\mathbf{X}^h(n) + \mathbf{F}_c = [\theta_c][\theta_h]\,\mathbf{X}^c(n) + \mathbf{F}_c + [\theta_c]\mathbf{F}_h \tag{33}$$

where $[\theta_h]$ and $[\theta_c]$ are bidiagonal matrices and $\mathbf{F}_h$ and $\mathbf{F}_c$ are column vectors representing the feed contribution. Table 1 below gives the elements of these matrices and vectors, corresponding to the stages in which the conservation and equilibrium relations are written. All other elements are zero.

x_F is the feed composition, assumed constant here. The feed vectors $\mathbf{F}_h$ and $\mathbf{F}_c$ have each a single nonzero element, owing to the fact that the feed is added in a given single stage. The nonzero element is not on the same line in the two vectors because the feed is mixed with a different mobile-phase fraction in

TABLE 1

Index of stage	Stage or reservoir	$(\rho + \alpha^h)[\theta_h]$ Main diagonal	$(\rho + \alpha^h)[\theta_h]$ Upper diagonal	$(\rho + \alpha^h)\mathbf{F}_h$	$(\rho + \alpha^c)[\theta_c]$ Main diagonal	$(\rho + \alpha^c)[\theta_c]$ Lower diagonal	$(\rho + \alpha^c)\mathbf{F}_c$
	Top reservoir				$\rho + \alpha^c$		0
$1, 2, \ldots, f-1$	Stage in top section	$\rho - \gamma_h$	$\alpha^c + \gamma_h$	0	ρ	α^h	0
f (feed)	Feed stage	$\rho - \gamma_h$	α^c	$\gamma_h x_F$	$\rho - \gamma_c$	α^h	$\gamma_c x_F$
$f+1, f+2, \ldots, N$	Stage in bottom section	ρ	α^c	0	$\rho - \gamma_c$	$\alpha^h + \gamma_c$	0
	Bottom reservoir	$\rho + \alpha^h$		0			

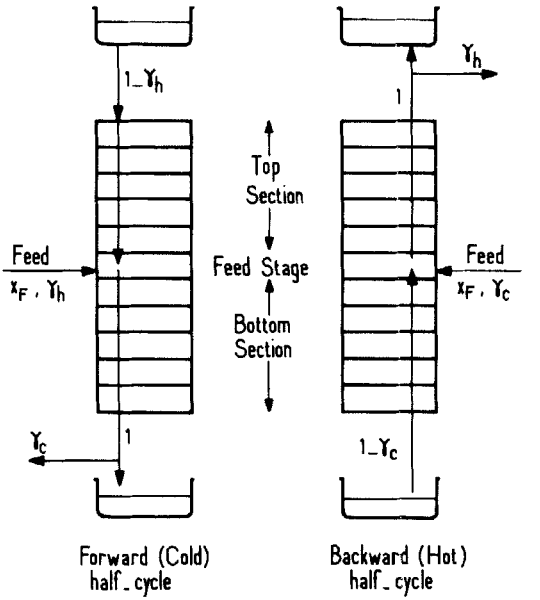

FIG. 10. Operating scheme of partial reflux staged parapump.

the hot and cold steps. Note that a feed distributed over several stages can be accounted for by the same Eqs. (32) and (33), but different elements in the matrices $[\theta_h]$ and $[\theta_c]$, and additional nonzero elements in $\mathbf{F}_c$ and $\mathbf{F}_h$.

The general solution of the first-order recurrence of Eqs. (32) and (33), relating $\mathbf{X}^c(n+1)$ to $\mathbf{X}^c(n)$, is easily seen to be

$$\mathbf{X}^c(n) = [\mathbf{M}]^n \mathbf{X}^c(0) + [\mathbf{I} + \mathbf{M} + \mathbf{M}^2 + \ldots + \mathbf{M}^{n-1}][\mathbf{F}_c + [\theta_c]\mathbf{F}_h] \tag{34}$$

where $[\mathbf{M}] = [\theta_c][\theta_h]$. Equation (34) is to be compared to Eq. (14) (note that $[\mathbf{M}]$ is not the same in these two equations). The matrix $[\mathbf{M}]$ is still tridiagonal and the methods for calculating the eigenvalues remain valid. The geometric matrix series $[\mathbf{I} + \mathbf{M} + \mathbf{M}^2 + \cdots + \mathbf{M}^{n-1}]$ can be rewritten by applying Sylvester's theorem (Eqs. 19 and 20) to each term, so that a scalar geometric series appears on each eigenvalue. If all λ's are different from 1, Eq. (34) becomes

$$\mathbf{X}(n) = \sum_{j=0}^{N} [\mathbf{A}_j] \left[\lambda_j^n \mathbf{X}(0) + \frac{1 - \lambda_j^n}{1 - \lambda_j} \mathbf{F} \right] \tag{35}$$

where $[\mathbf{A}_j]$ are matrices obtained from $[\mathbf{M}]$ by applying Eq. (20) and $\mathbf{F}$ is the overall feed vector, given by

$$\mathbf{F} = \mathbf{F}_c + [\theta_c]\mathbf{F}_h = \frac{x_F}{(\rho + \alpha^c)(\rho + \alpha^h)} \begin{bmatrix} 0 \\ \cdot \\ \cdot \\ \cdot \\ 0 \\ \rho\gamma_h \\ \gamma_c(\rho + \alpha^h) + \gamma_h\alpha^h \\ 0 \\ \cdot \\ \cdot \\ \cdot \\ 0 \end{bmatrix}$$

the two nonzero elements of $\mathbf{F}$ are on lines f and $f+1$.

If any eigenvalue was larger than or equal to 1, the series $\mathbf{I} + \mathbf{M} + \cdots + \mathbf{M}^{n-1}$ would not converge and no steady state would be reached. On physical grounds, we may thus state that all eigenvalues are smaller than 1. Under these conditions the cyclic steady state is not obtained directly as an eigenvector of $[\mathbf{M}]$, but by letting $\mathbf{X}(n+1) = \mathbf{X}(n)$ in Eq. (33) or $n \to \infty$ in Eq. (35):

$$\mathbf{X}^c(\infty) = [\mathbf{I} - \mathbf{M}]^{-1}\mathbf{F} = \sum_{j=0}^{N} \frac{[\mathbf{A}_j]}{1 - \lambda_j}\mathbf{F} \tag{36}$$

We know from a previous publication (*9*) that the cyclic steady state can be geometrically represented by a McCabe-Thiele diagram somewhat more complicated than that of total reflux (Figs. 6a and 6b), and that the analytical expressions for the separation factor are quite involved. There is thus little hope to bring Eq. (36) to a more analytical form by simple manipulations.

APPENDIX A: CALCULATION OF EIGENVALUES OF $|\mathbf{M}|$ *(20)*

The eigenvalues of $[\mathbf{M}]$ are calculated from the equation

$$P_M(\lambda) = \det|\mathbf{M} - \lambda\mathbf{I}| = \begin{bmatrix} d-p\lambda & e & 0 & 0 & 0 & 0 \\ a & b-p\lambda & c & 0 & 0 & 0 \\ 0 & a & b-p\lambda & c & 0 & 0 \\ 0 & 0 & a & b-p\lambda & c & 0 \\ 0 & 0 & 0 & a & b-p\lambda & c \\ 0 & 0 & 0 & 0 & a & a+b-p\lambda \end{bmatrix} = 0 \tag{A1}$$

Since the determinant is tridiagonal, it may be expanded easily by elements of the last column for example. Let $P_{N-1}(\lambda)$ be the determinant obtained by

deleting the last row and the last column, and let $P_{N-j}(\lambda)$ be the determinant obtained by deleting the j last rows and columns. We then have (with $N = 6$)

$$\begin{aligned}
P_6(\lambda) &= (a + b - p\lambda)P_5(\lambda) - acP_4(\lambda) \\
P_5(\lambda) &= (b - p\lambda)P_4(\lambda) - acP_3(\lambda) \\
P_4(\lambda) &= (b - p\lambda)P_3(\lambda) - acP_2(\lambda) \\
P_3(\lambda) &= (b - p\lambda)P_2(\lambda) - acP_1(\lambda) \\
P_2(\lambda) &= (b - p\lambda)P_1(\lambda) - acP_0(\lambda) \\
P_1(\lambda) &= (d - p\lambda)P_0(\lambda) \\
P_0(\lambda) &= 1
\end{aligned} \tag{A2}$$

A trial value of λ is assumed and the successive expressions $P_i (i = 1 \text{ to } N)$ are calculated. An eigenvalue is found when $P_N(\lambda) = 0$.

The localization of the eigenvalues, and thus the trial values, is facilitated by the fact that the expressions P_i form a Sturm series which permits the following test: Assume a value λ' and calculate the sequence $P_0 \ldots P_N$. Let $V(\lambda')$ be the number of sign changes in this series. Assume another trial value λ'' and determine in the same way the number of sign changes in the sequence $V(\lambda'')$. The difference $V(\lambda') - V(\lambda'')$ gives the number of real eigenvalues in the interval (λ', λ''). This property may be used to show that all eigenvalues are real. We assume λ' very large and positive and λ'' very large and negative. It is then easy to see that

$\lambda' \gg 0$	$\lambda'' \ll 0$
$P_0 = 1 > 0$	$P_0 = 1 > 0$
$P_1 = d - p\lambda < 0$	$P_1 = d - p\lambda > 0$
$P_2 = (b - p\lambda)P_1 - ac > 0$	$P_2 = (b - p\lambda)P_1 - ac > 0$
$P_3 < 0$	$P_3 > 0$
$P_4 > 0$	$P_4 > 0$
$P_5 < 0$	$P_5 > 0$
$P_6 > 0$	$P_6 > 0$

The numbers of sign changes are $V(\lambda') = N$ and $V(\lambda'') = 0$, and the number of real eigenvalues, positive or negative, is N. Thus all eigenvalues are real.

The Sturm sequence (A2) may also conveniently be used to show that $\lambda = 1$ is an eigenvalue. For $\lambda = 1$, we have

$$P_0 = 1 > 0$$
$$P_1 = d - p = -\alpha^h(\rho + \alpha^c) < 0$$
$$P_2 = (b - p)P_1 - ac = -aP_1$$
$$P_3 = (b - p)P_2 - acP_1 = -aP_2 - cP_2 - acP_1 = -aP_2$$
$$P_j = (b - p)P_{j-1} - acP_{j-2} = -aP_{j-1} - cP_{j-1} - acP_{j-2}$$

and since

$$P_{j-1} = -aP_{j-2}$$

we have

$$P_j = -aP_{j-1}$$

For the last polynomial P_N, which represents the characteristic equation, we have

$$P_N = (a + b - p)P_{N-1} - acP_{N-2}$$

with

$$a + b - p = -c$$

and

$$P_{N-1} = -aP_{N-2}$$

thus

$$P_N = 0$$

and $\lambda = 1$ satisfies the characteristic equation and is thus an eigenvalue, independent of the values of the parameters. Incidentally, this calculation shows that $V(\lambda'' = 1) = N - 1$. Since $V(\lambda' \gg 0) = N$, there is a single real root in the interval $(+1, +\infty)$ which is precisely $\lambda = 1$. No eigenvalue can thus have a value larger than 1. A somewhat more tedious calculation can be made for $\lambda'' = 0$, showing that $V(\lambda'' = 0) = 0$. This ensures that all eigenvalues are positive, and finally, we must have

$$0 < \lambda_0 < \lambda_1 < \cdots < \lambda_N = 1$$

APPENDIX B: THE STRUCTURE OF $[\mathbf{M}]^\infty$

For large values of n, that is, at cyclic steady state, $[\mathbf{M}]^n$ must satisfy the $N + 1$ equations

$$[\mathbf{M}]^n\mathbf{X}(0) = \mathbf{X}(\infty) \tag{B1}$$

independently of the initial distribution $\mathbf{X}(0)$. The concentrations $(q_0, q_1, \ldots, q_N)$ of $\mathbf{X}(0)$, and the concentration $(x_0^*, x_1^*, \ldots, x_N^*)$ of $X(\infty)$ are related only by the condition of conservation of the mass of solute in the whole system. This condition is expressed by:

$$Q = W\left[\rho q_0 + \sum_{i=1}^{N}(\rho + \alpha^c)q_i\right] = W\left[\rho x_0^* + \sum_{i=1}^{N}(\rho + \alpha^c)x_i^*\right] \tag{B2}$$

Replacing x_i^* by $x_0^*\beta^{-i}$ from Eq. (24), factoring out x_0^* in the right-hand side, and reorganizing, we obtain

$$Aq_0 + B\sum_{i=1}^{N} q_j = x_0^* \tag{B3}$$

where

$$A = \frac{\rho}{\rho + (\rho + \alpha^c)\sum_{k=1}^{N}\beta^{-k}}; \qquad B = \frac{\rho + \alpha^c}{\rho}A \tag{B4}$$

Clearly the $N + 2$ equations (B1) and (B3) may hold for any set of q_j only if they are redundant. We may thus identify, for example, (B3) with the ith equation of (B1), which we write $(i = 0, 1, \ldots, N)$

$$m_{i0}q_0 + m_{i1}q_1 + \ldots + m_{iN}q_N = x_i^* = x_0^*\beta^{-i} \tag{B4}$$

and we obtain

$$m_{ij}\beta^i = \begin{cases} A \text{ for } j = 0 \\ B \text{ for } j = 1, \ldots, N \end{cases} \tag{B6}$$

The elements m_{ij} of $[\mathbf{M}]^\infty$ are thus completely identified by Eq. (B6), together with (B4). $[\mathbf{M}]^n$ may be visualized as

$$[\mathbf{M}]^\infty = \begin{vmatrix} A & B & B \ldots\ldots\ldots\ldots\ldots B \\ A\beta^{-1} & B\beta^{-1} & B\beta^{-1} \ldots\ldots\ldots\ldots\ldots B\beta^{-1} \\ A\beta^{-2} & B\beta^{-2} & B\beta^{-2} \ldots\ldots\ldots\ldots\ldots B\beta^{-2} \\ \cdot & & \cdot \\ \cdot & & \cdot \\ \cdot & & \cdot \\ A\beta^{-N} & B\beta^{-N} \ldots\ldots\ldots\ldots\ldots\ldots B\beta^{-N} \end{vmatrix} \tag{B7}$$

It may be verified that this matrix is invariant on multiplication on the left or on the right by [**M**].

It is interesting to look at the other possible approach starting from Eq. (17):

$$[\mathbf{M}]^{\infty} = [\mathbf{P}][\Lambda]^{\infty}[\mathbf{P}^{-1}] \tag{B8}$$

Clearly Λ^{∞} reduces to the single element 1 in the last row and last column, all other elements being zero. The product $[\mathbf{P}][\Lambda]^{\infty}$ is a matrix with the first N columns of zeroes, the last column being the last column of [**P**]; that is, the eigenvector belonging to $\lambda = 1$. Multiplying this matrix by $[\mathbf{P}^{-1}]$, we should recover the result of Eq. (B7). It is easy to show that the only elements of $[\mathbf{P}^{-1}]$ that appear in the product are the elements of the last row, which are the cofactors of the above-mentioned eigenvector in [**P**]. Identifying with (B7), we conclude that the last row of $[\mathbf{P}^{-1}]$ is $(ABB \ldots B)$.

SYMBOLS

a, b, c, d, e, p	coefficients in material balance equations, defined by Eq. (13) (dimensionless)
A, B	quantities defined by Eq. (B4) (Appendix B)
m_{ij}	elements of matrix $[\mathbf{M}]^{\infty}$, defined in Appendix B (dimensionless)
n	number of cycles (dimensionless)
N	total number of stages (dimensionless)
$P_i(\lambda)$	minor determinants of matrix $(\mathbf{M} = \lambda\mathbf{I})$, defined by Eq. (A2) (Appendix A) (dimensionless)
$q_0, q_1, \ldots, q_N$	initial values of $x_0, x_1, \ldots, x_N$ (g/L)
Q	total mass of phenol present in the system (g)
T	volume of toluene fractions (L)
W	volume of water fractions (L)
$x_j(n)$	phenol concentration in toluene (mobile phase) fraction number j ($j = 0, 1, \ldots, N$), in cycle number n (g/L)
x_j^*	values of x_j in cyclic steady state (g/L)
x_{ik}	ith component of the kth eigenvector ($i = 1, 2, \ldots, N$; $k = 0, 1, \ldots, N$) defined by Eq. (15) (g/L)
x_F	phenol concentration in feed for open parapump (g/L)
$y_k(n)$	phenol concentration in water (stationnary phase) in stage number k ($k = 1, 2, \ldots, N$) and in cycle number n (g/L)

Greek Letters

α^c, α^h	slopes of the equilibrium isotherms (concentration in water versus concentration in toluene) at the cold and the warm temperature, respectively (dimensionless)
β	relative thermal affinity defined by Eq. (24) (dimensionless)
γ	dead volume ratio, defined by Eq. (30) (dimensionless)
$\lambda_0, \lambda_1, \ldots, \lambda_N$	eigenvalues of matrix [**M**] (dimensionless)
ρ	ratio of volumes of toluene fraction to water fraction defined by Eq. (2) (dimensionless)

Vector and Matrix Quantities

$[\mathbf{A}_j]$	matrices defined by Eq. (20)
$\mathbf{C}$	column vector defined by Eq. (29)
$\mathbf{F}_c$, $\mathbf{F}_h$	feed vectors in open parapump, defined by Eqs. (33)
$[\mathbf{I}]$	unity matrix
$[\mathbf{M}]$, $[\theta]$	matrices of coefficients in material balance equations, defined by Eqs. (8), (10), and (12)
$[\mathbf{P}]$, $[\mathbf{P}^{-1}]$	matric of column eigenvectors of [**M**], and inverse
$\mathbf{X}$	column vector of phenol concentrations in toluene fractions $(x_0, x_1, \ldots, x_N)$
$[\Lambda]$	diagonal matrix of eigenvalues

Indices, Subscripts, and Superscripts

*, (∞)	define the cyclic steady-state
c, h	designate variables defined at the cold temperature and at the hot temperature, respectively
(n)	number of cycles
i, j, k	refer to number of a toluene or water fraction

REFERENCES

1. R. H. Wilhelm, A. W. Rice, and A. R. Bendelius, *Ind. Eng. Chem., Fundam.*, 5, 141 (1966).
2. N. H. Sweed, in *Recent Developments in Separation Science*, Vol. 1 (N. Li, ed.), Chemical Rubber Co., Cleveland, Ohio, 1972.
3. P. C. Wankat, *Sep. Sci.*, 9, 85 (1974).
4. R. G. Rice, *Sep. Purif. Methods*, 5, 139 (1976).
5. P. C. Wankat, *Ind. Eng. Chem., Fundam.*, 12, 372 (1973).

6. N. Wakao et at., *Kagaku Kogaku, 32*, 169 (1968).
7. G. Grevillot and D. Tondeur, *AIChE J., 22*, 1055 (1976).
8. G. Grevillot and D. Tondeur, *Ibid., 23*, 840 (1977).
9. G. Grevillot, *Ibid., 26*, 120 (1980).
10. L. C. Craig and D. Craig, *Techniques of Organic Chemistry,* Vol. 3 (A. Weissberger, ed.), Interscience, New York, 1956, p. 149.
11. L. C. Craig, *Anal. Chem., 22,* 61 (1950).
12. L. C. Craig, *Ibid., 23*, 41 (1951).
13. L. C. Craig, *Ibid., 24*, 66 (1952).
14. L. C. Craig, *Ibid., 26*, 110 (1954).
15. L. C. Craig, H. Werner, H. Hedward, Jr., J. R. Ahrens, and E. J. Harfenst, *Ibid., 23*, 1236 (1951).
16. L. C. Craig and O. Post, *Ibid., 25*, 500 (1949).
17. R. E. Treybal, *Liquid Extraction*, McGraw-Hill, New York, 1955.
18. H. L. Lochte and H. W. Meyer, *Anal. Chem., 22*, 1064 (1950).
19. O. Post and L. C. Craig, *35*, 641 (1963).
20. N. R. Amundson, *Mathematical Methods in Chemical Engineering. Vol. 1. Matrices and Their Applications*, Prentice-Hall, Englewood Cliffs, New Jersey, 1966.
21. R. L. Pigford, B. Baker, and D. E. Blum, *Ind. Eng. Chem., Fundam., 8*, 144 (1969).

Received by editor May 22, 1981